

Searching Dense Point Correspondences via Permutation Matrix Learning

Zhiyuan Zhang¹, Jiadai Sun¹, Yuchao Dai¹, Bin Fan¹, and Qi Liu¹

Abstract—Although 3D point cloud data has received widespread attentions as a general form of 3D signal expression, applying point clouds to the task of dense correspondence estimation between 3D shapes has not been investigated widely. Furthermore, even in the few existing 3D point cloud-based methods, an important and widely acknowledged principle, *i.e.* one-to-one matching, is usually ignored. In response, this paper presents a novel end-to-end learning-based method to estimate the dense correspondence of 3D point clouds, in which the problem of point matching is formulated as a zero-one assignment problem to achieve a permutation matching matrix to implement the one-to-one principle fundamentally. Note that the classical solutions of this assignment problem are always non-differentiable, which is fatal for deep learning frameworks. Thus we design a special matching module, which solves a doubly stochastic matrix at first and then projects this obtained approximate solution to the desired permutation matrix. Moreover, to guarantee end-to-end learning and the accuracy of the calculated loss, we calculate the loss from the learned permutation matrix but propagate the gradient to the doubly stochastic matrix directly which bypasses the permutation matrix during the backward propagation. Our method can be applied to both non-rigid and rigid 3D point cloud data and extensive experiments show that our method achieves state-of-the-art performance for dense correspondence learning.

Index Terms—Dense correspondence estimation, One-to-one matching, Point cloud, End-to-end learning.

I. INTRODUCTION

As a new form of 3D signal expression, point cloud has received widespread attention due to the talent for representing 3D shapes efficiently and being obtained directly and easily by scanning. And it has been adopted in many applications, such as segmentation [1], [2], 3D reconstruction [3], [4], compression [5]–[7], autonomous driving [8]. Particularly, although dense correspondence estimation is a fundamental task in computer vision, which has been investigated widely on other signal formats (*e.g.* 2D image [9], [10]), it remains a challenging problem for point cloud data due to the inherent characteristics of the point cloud (*e.g.* irregularity, orderless), the serious deformation of object shape, and so on. Note that most existing methods of 3D shape correspondence estimation pay more attention to the 3D mesh input [11]. And although many 3D mesh-based methods have been encouraged [12]–[16], these methods cannot be extended to 3D point cloud

input directly since there is no topology information existing in 3D point cloud comparing with the 3D mesh.

To solve the correspondence searching problem for the 3D point clouds directly, scene flow estimation methods *e.g.* FlowNet3D [17], are usually borrowed by selecting the nearest point as the corresponding point. However, an important and widely acknowledged principle, *i.e.* one-to-one matching, is ignored. This will result in a large number of one-to-many matches and unsatisfactory performance. CorrNet3D [18] is a representative method advocating solving a permutation matching matrix to ensure the one-to-one matching. However, this intention is not realized because the learned matching matrix is still a soft probability matrix and the final corresponding point is determined by selecting the point with the largest matching probability where the one-to-many matching is still not excluded. Besides, as a special task, learning point correspondence between rigid point clouds has been broadly investigated as a crucial intermediate step in the point cloud registration field [19]. However, most of them [20]–[23] advocate building some reliable correspondences, which is reasonable for registration but do not make sense for dense correspondence estimation task. Some virtual point-based methods [24], [25] advocate estimating dense correspondence, however, the learned correspondence is not accurate since the constructed virtual points degenerate seriously. In summary, as far as we know, the one-to-one matching principle has not been implemented well in the existing 3D point cloud-based dense correspondence learning methods.

In this paper, we focus on the dense correspondence estimation problem of 3D shapes in the form of point clouds and achieve the real one-to-one matching learning in an end-to-end manner for the first time. To this end, we formulate the point matching as a zero-one assignment problem to solve a special binary matrix, permutation matrix (PM)¹ to implement one-to-one matching principle fundamentally. Although the binary matrix has been investigated widely in [26], [27], the desired PM further constrains the sum of each row and column. Note that the classical solutions of the assignment problem are always not differentiable [28], which is fatal for deep learning frameworks. In response, a special matching module is designed. This module firstly solves a doubly stochastic matrix (DSM) as the approximate solution and then projects the obtained DSM to the desired PM. Moreover, to guarantee the end-to-end learning and the accuracy of the calculated loss, we advocate calculating the loss from the learned PM but propagating the gradient to the DSM directly during the backward

This work was supported in part by the National Key Research and Development Program of China (2018AAA0102803) and National Natural Science Foundation of China (61871325, 61901387), and Innovation Foundation for Doctor Dissertation of Northwestern Polytechnical University (CX2022046).

¹School of Electronics and Information, Northwestern Polytechnical University, Xi'an, 710129, China. Yuchao Dai is the corresponding author, Email: daiyuchao@nwpu.edu.cn.

¹The formal definitions of PM, DSM are given in the following section.

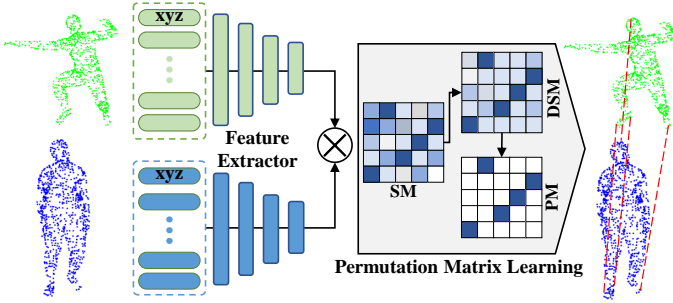


Fig. 1: The outline of the proposed dense correspondence learning framework. For the input 3D point clouds, the point features are extracted at first, and then the one-to-one matching is achieved by learning a permutation matching matrix.

propagation. Our method can be employed to both non-rigid and rigid point cloud data. Extensive evaluations on several benchmark datasets validate that our method achieves state-of-the-art performance for dense correspondence learning.

Our contributions can be summarized as follows: 1). We propose to learn the permutation matching matrix in an end-to-end learning to implement one-to-one principle fundamentally. 2). Our method can handle both non-rigid and rigid 3D point clouds directly for dense correspondence estimation. 3). Extensive evaluations validate the superiority of our method, which creates a new state-of-the-art performance.

II. METHOD

In this section, our dense correspondence learning approach is introduced in detail. The outline is illustrated in Fig. 1.

A. Preliminaries

Given the *source* point cloud $\mathbf{X} = [\mathbf{x}_i] \in \mathbb{R}^{3 \times N}$ and the *target* point cloud $\mathbf{Y} = [\mathbf{y}_j] \in \mathbb{R}^{3 \times N}$, which represent the same deformable 3D shape, we aim at estimating the dense point-to-point correspondence in this paper. Specifically, the matching matrix $\mathbf{M} = [m_{ij}] \in \{0, 1\}^{N \times N}$ is searched to indicate the assignment between the points in \mathbf{X} and \mathbf{Y} , where $m_{ij} = 1$ if point \mathbf{x}_i in \mathbf{X} and point \mathbf{y}_j in \mathbf{Y} are matched, and $m_{ij} = 0$ otherwise. The desired \mathbf{M} is equivalent to PM, *i.e.* $\sum_{i=1}^N m_{ij} = 1, \forall j$, $\sum_{j=1}^N m_{ij} = 1, \forall i$ and $m_{ij} \in \{0, 1\}$, by which the one-to-one matching principle can be formulated.

B. Feature Extractor

For accurate matching, distinguished descriptors are crucial. Currently, deep features have been widely used. In our method, we apply “DGCNN + Transformer” as the feature extractor. Specifically, a DGCNN [29] is firstly employed to compute the initial point features, which incorporates the neighbor information in both 3D Euclidean space and feature space. Besides, inspired by the recent success of the attention mechanism, we use Transformer [30] to learn cross-contextual information for more descriptive point features. Formally, we denote the DGCNN feature as $\mathbf{F}_\mathbf{X} = [\mathbf{F}_{\mathbf{x}_i}] \in \mathbb{R}^{N \times d}$, d is the pre-defined feature dimension. Analogously, $\mathbf{F}_\mathbf{Y} = [\mathbf{F}_{\mathbf{y}_j}] \in \mathbb{R}^{N \times d}$. Then, the Transformer is applied, *i.e.* $\Phi_\mathbf{X} = \mathbf{F}_\mathbf{X} + \eta(\mathbf{F}_\mathbf{X}, \mathbf{F}_\mathbf{Y})$, $\Phi_\mathbf{Y} = \mathbf{F}_\mathbf{Y} + \eta(\mathbf{F}_\mathbf{Y}, \mathbf{F}_\mathbf{X})$, where $\eta: \mathbb{R}^{N \times d} \times \mathbb{R}^{N \times d} \rightarrow \mathbb{R}^{N \times d}$ is the Transformer function. The final point features of all *source* points and *target* points are represented as $\Phi_\mathbf{X} = [\Phi_{\mathbf{x}_i}] \in \mathbb{R}^{N \times d}$ and $\Phi_\mathbf{Y} = [\Phi_{\mathbf{y}_j}] \in \mathbb{R}^{N \times d}$.

C. Permutation Matrix Learning

As mentioned above, we devote to learning a permutation matrix to implement one-to-one principle fundamentally. To this end, we design a dedicated matching module as follows to guarantee the end-to-end learning.

Initial similarity matrix solving. In our matching module, we firstly compute an initial similarity matrix (SM). Based on the obtained deep features $\Phi_\mathbf{X}$ and $\Phi_\mathbf{Y}$, the SM \mathbf{S} is calculated by using the scale dot product attention metric [30], *i.e.* $\mathbf{S} = \Phi_\mathbf{X} \Phi_\mathbf{Y}^\top / \sqrt{d}$, where the entry s_{ij} represents the similarity between point \mathbf{x}_i in \mathbf{X} and point \mathbf{y}_j in \mathbf{Y} .

Permutation matrix Learning. Note that the SM \mathbf{S} is in continuous space while the desired PM \mathbf{M} is in discrete space with the entry of either 0 or 1, solving PM can be defined as a zero-one assignment problem whose existing solutions are always non-differentiable. Therefore, how to optimize \mathbf{S} to \mathbf{M} in a deep learning pipeline is the main challenge. To solve this problem, we design an ingenious matching method as presented in Alg. 1. And a DSM \mathbf{P} is solved as an intermediate variable between \mathbf{S} and \mathbf{M} as shown in Fig. 1, where $\mathbf{P} = [p_{ij}] \in [0, 1]^{N \times N}$, $\sum_{i=1}^N p_{ij} = 1, \forall j$, $\sum_{j=1}^N p_{ij} = 1, \forall i$. Firstly, this two-stage method applies the Gumbel-Sinkhorn algorithm [31] to solve \mathbf{P} as an approximate solution of \mathbf{M} . Compared to the original Sinkhorn method, the Gumbel-Sinkhorn is more robust by adding a standard i.i.d. Gumbel noise matrix ϵ to the input \mathbf{S} . Then, \mathbf{P} is projected to the final permutation matching matrix \mathbf{M} by formulating a zero-one assignment problem, in which objective function is defined by considering the DSM \mathbf{P} as the profit matrix, *i.e.*

$$\mathbf{M}^* = \arg \max_{\mathbf{M} \in \mathcal{M}_N} \langle \mathbf{M}, \mathbf{P} \rangle_F, \quad (1)$$

where \mathcal{M}_N denotes the set of permutation matrices and $\langle \mathbf{M}, \mathbf{P} \rangle_F = \text{trace}(\mathbf{M}^\top \mathbf{P})$ denotes the (Frobenius) inner product of matrices. There are many classical solutions to this assignment problem. In our implementation, the representative Hungarian algorithm [28] is applied.

Algorithm 1: Permutation Matrix Learning.

Input: Initial similarity matrix \mathbf{S} , Gumbel noise matrix ϵ , Hyper-parameter μ , iteration number $Iter$.

Output: Optimal Permutation Matrix \mathbf{M}^* .

$\mathbf{S} = ((\mathbf{S} + \epsilon) / \mu)$; // add Gumbel noise to similarity matrix

$\mathbf{S} = \exp(\mathbf{S})$;

while $it \leq Iter$ **do**

$\mathbf{S} = \mathcal{T}_r(\mathbf{S})$; // \mathcal{T}_r indicates row-wise normalization

$\mathbf{S} = \mathcal{T}_c(\mathbf{S})$; // \mathcal{T}_c indicates column-wise normalization

$\mathbf{P} = \mathbf{S}$; // \mathbf{P} is the DSM returned by final \mathbf{S} .

$\mathbf{M}^* = h(\mathbf{P})$. // $h(\cdot)$ indicates the Hungarian algorithm

D. Loss Function

Here, we supervise the learned matching matrix directly. Specifically, the loss function is defined as

$$\mathcal{L} = -\frac{1}{N} \sum_{i=1}^N \sum_{j=1}^N \left(m_{ij}^{\text{pred}} m_{ij}^{\text{gt}} \right), \quad (2)$$

where the superscript “pred” and “gt” indicate the prediction and the ground truth, respectively.

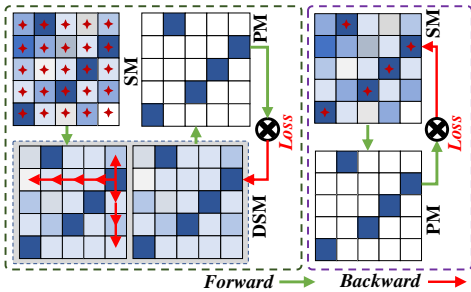


Fig. 2: The illustration of forward and backward propagation in our two-stage matching module (Left) and one-stage matching module (Right). Our method not only guarantees the end-to-end learning but also avoids the local supervision risk.

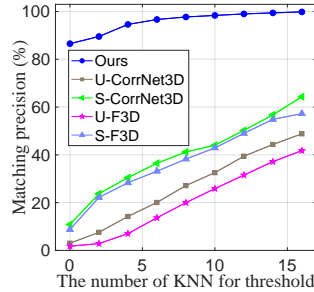
E. Remarks

Here, we stress the ingenuity of the designed PM learning module in the end-to-end learning pipeline. As mentioned above, this zero-one assignment problem is fatal for the deep learning pipeline due to the non-differentiability. As a response, we propose an ingenious operation as shown in Fig. 2 Left. Specifically, during the forward propagation, the loss is calculated based on the learned PM M . However, during the backward propagation, the gradient is propagated to the learned DSM P directly bypassing the PM solving procedure. This operation guarantees the accuracy of the calculated loss and the end-to-end training synchronously.

Then, a natural question is that, *since the assignment procedure is bypassed in backward propagation, why not use the similarity matrix as the profit matrix to solve the permutation matrix but use DSM as the profit matrix*. Although this one-stage strategy is more direct as shown in Fig. 2 Right, it exists an obvious local supervision risk. Specifically, if the gradient is propagated to the SM directly, the correlation of entries, which should have been considered in the assignment algorithm, is ignored in backward propagation, *i.e.* the loss calculated from m_{ij} can only supervise s_{ij} . Note that, from Eq. (2), when $m_{ij}^{gt} = 1$, m_{ij}^{pred} is enforced to 1. When $m_{ij}^{gt} = 0$, m_{ij}^{pred} is trained without supervision. Thus many entries ($N(N-1)$) will be trained without supervision in this one-stage method, and the training will not converge. Our solution avoids this local supervision risk effectively by propagating the gradient to the intermediate DSM, where the correlation of all entries is considered again in Gumbel-Sinkhorn. Through our method, the similarity of the correct correspondences will be boosted, meanwhile the similarity of the wrong correspondences will be effectively suppressed during the backward propagation.

III. EXPERIMENTAL RESULTS

We conduct extensive experiments on both non-rigid and rigid point cloud. In our application, in the feature extractor, a 4-layer graph neural network is applied where the parameter of K-nearest neighbor is set to 24, the embedding dimension $d = 512$, iteration number $Iter = 5$, hyper-parameter $\mu = 0.5$. As for the training, we at first train the feature extractor with an incomplete pipeline, *i.e.* solving DSM only without assignment for 100 epochs. Then, we insert the Hungarian algorithm, and retrain the entire network for 100 epochs. The initial learning rate in the Adam optimizer is set to 0.001.



Method	F\F	S\S	F\S	S\F
BCICP	15.	16.	*	*
ZoomOut	6.1	7.5	*	*
SURFMNet	15.	12.	32.	32.
SURFMNet+icp	7.4	6.1	19.	23.
U-FMNet	10.	16.	29.	22.
U-FMNet+pmf	5.7	10.	12.	9.3
FMNet	11.	17.	30.	33.
FMNet+pmf	5.9	6.3	11.	14.
3D-CODED	2.5	31.	31.	33.
DeepGFM	3.1	4.4	11.	6.0
DeepGFM+zo	1.9	3.0	9.3	4.3
Ours	1.7	4.6	9.3	5.2

Fig. 3: Comparison of the TABLE I: Comparison of per-matching precision for non-point-average geodesic distance rigid 3D point clouds on results ($\times 100$). Four dataset sets-Surreal\SHREC. And $K =$ tings are evaluated, which are 0 means the threshold is 0. indicated by **train set\test set**.

Datasets. For non-rigid shape correspondence, following [18], we adopted Surreal [32] and SHREC [14] as the training and test sets respectively. Besides, the re-meshed versions of FAUST [33] and SCAPE [34] are also used following [35]. For all mesh data, our method randomly picked vertices as the point cloud. For rigid shape correspondence, ModelNet40 [36] is used following the registration methods [24], [25].

Metrics. We use the matching precision (%) metric here to evaluate the dense correspondence estimation performance. Theoretically, it presents the correct correspondence percentage by $\frac{1}{N} \|\mathbf{M}^{pred} \odot \mathbf{M}^{gt}\|_1$, where \odot is the Hadamard product, \mathbf{M}^{pred} , \mathbf{M}^{gt} represent the predicted and ground truth matching matrices, respectively. In actual application, this metric is often relaxed by confirming the correspondence as a correct result when the distance between the predicted corresponding point and the real corresponding point is less than a threshold. Here, we propose a self-adaptive threshold as $\tau_i = \frac{1}{K} \sum_{j=1}^K l_{\mathbf{x}_i, \mathbf{x}_j}$, $\mathbf{x}_j \in \text{KNN}(\mathbf{x}_i)$, where $l_{\mathbf{x}_i, \mathbf{x}_j}$ is the Euclidean distance between the points \mathbf{x}_i and \mathbf{x}_j , $\text{KNN}(\cdot)$ represents the K-nearest neighbor. In other words, for i -th point \mathbf{x}_i , τ_i is computed as the mean distance of K nearest neighbor points. Meanwhile, for a fair comparison, the metric of per-point-average geodesic distance [14] is also used for the methods with 3D mesh input.

Comparison methods: For non-rigid shape correspondence estimation, we first compare with point cloud-based methods including FlowNet3D [17], CorrNet3D [18], in Unsupervised and Supervised training, notated as U-F3D, S-F3D, U-CorrNet3D and S-CorrNet3D respectively. Then, 3D mesh-based methods are also compared, including traditional methods ZoomOut [37], BCICP [38], and learning-based methods 3D-CODED [32], FMNet [12], U-FMNet [13] with and without post-processing (PMF [39]), SURFMNet [40] with and without ICP, DeepGFM [14] with and without ZoomOut (ZO). For rigid input, ICP [41], DCP [24], PRNet [23] are evaluated. For PRNet, two versions have been evaluated here. For the original version, which is denoted as PRNet, half input points are selected as key points. For the modified version, which is denoted as PRNet*, all points are considered as key points for dense correspondence.

A. Evaluation on Non-rigid Data

Fig. 3 shows the quantitative comparison with 3D point clouds input on Surreal\SHREC. Our method always pro-

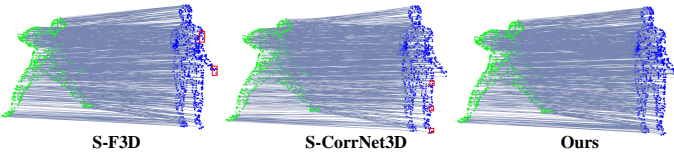


Fig. 4: Matching results on SHREC, where green and blue represent the *source* and *target* respectively. The points which are not assigned corresponding points (indicated by the red box) show that one-to-many matching exists in baselines.

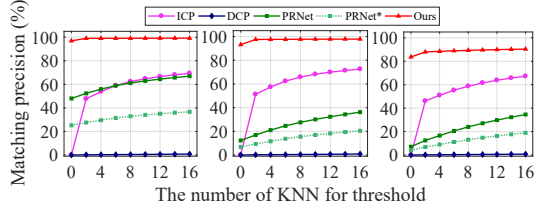


Fig. 5: Matching precision on rigid data. Three sub-figures indicate three settings, *i.e.* *UPC*, *UC* and *ND*. Obviously, our method outperforms baselines with a big margin.

duces the best performance under different thresholds, which outperforms all baselines by a large margin. Meanwhile, S-CorrNet3D achieves second-top results, which is better than S-F3D. We speculate that the large deformation of input shapes is difficult for scene flow estimation. Besides, we present a qualitative comparison in Fig. 4. Here, we indicate some points by the red box which are not assigned the corresponding points. Note that the input point clouds are in one-to-one correspondence, thus the problem of one-to-many matching exists in baselines. Our method achieves the real one-to-one matching with high matching precision.

For a fair comparison, the proposed method is compared with those 3D mesh-based methods on re-meshed FAUST and SCAPE. Here, we use the vertices as our input point cloud. And the per-point-average geodesic distance results between the ground truth and predicted corresponding points are reported. Following [14], all results are multiplied by 100 for the sake of readability. From the Table. I, our method gives accurate results on all settings, which is comparable with the state-of-the-art method, DeepGFM [14] outperforming other baselines. Moreover, we speculate that when the deformation becomes more severe, *e.g.* SCAPE dataset, the mesh-based method DeepGFM is more effective, where the topology information plays a more important role.

B. Evaluation on Rigid Data

In this section, we evaluate the dense correspondence estimation on rigid point clouds. For a comprehensive comparison, we also report the rigid transformation estimation results.

Following [24], [25], three different experiment settings are employed here. 1) Unseen point clouds (*UPC*): all the point clouds in the ModelNet40 are divided into training and test sets with the official setting. 2) Unseen categories (*UC*): in ModelNet40, we select the first 20 categories for training and the rest for testing. 3) Noisy data (*ND*): random Gaussian noise (*i.e.*, $\mathcal{N}(0, 0.01)$) is added to each point of input point clouds, while the sampled noise out of the range of $[-0.05, 0.05]$ will be clipped. The dataset split strategy is the same as *UPC*.

TABLE II: Evaluation of transformation estimation.

Method	RMSE(R)			MAE(R)			RMSE(t) ($\times 10^{-4}$)			MAE(t) ($\times 10^{-4}$)		
	<i>UPC</i>	<i>UC</i>	<i>ND</i>	<i>UPC</i>	<i>UC</i>	<i>ND</i>	<i>UPC</i>	<i>UC</i>	<i>ND</i>	<i>UPC</i>	<i>UC</i>	<i>ND</i>
ICP	12.282	12.707	11.971	4.613	5.075	4.497	477.44	485.32	483.20	22.80	23.55	23.35
FGR	20.054	21.323	18.359	7.146	8.077	6.367	441.21	457.77	391.01	164.20	18.07	144.87
PTLK	13.751	15.901	15.692	3.893	4.032	3.992	199.00	261.15	239.58	44.52	62.13	56.37
DCP-v2	1.094	3.256	8.417	0.752	2.102	5.685	17.17	63.17	318.37	11.73	46.29	233.70
PRNet	1.722	3.060	3.218	0.665	1.326	1.446	63.72	100.95	111.78	46.52	75.89	83.78
PRNet*	2.090	3.720	3.292	0.894	1.543	1.449	109.79	131.33	107.68	81.49	99.61	81.51
Ours	0.864	1.962	3.006	0.114	0.338	0.854	1.45	4.09	5.72	0.12	0.43	1.03

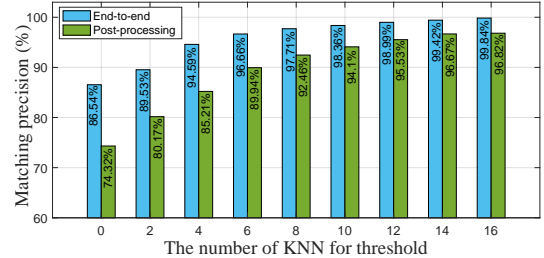


Fig. 6: Comparison of post-processing, end-to-end learning.

Correspondence estimation. We draw the matching precision in Fig. 5. The proposed method outperforms other state-of-the-art methods with a big margin. These obtained results are reasonable because the DCP-v2 is a virtual point-based method that fails to predict the corresponding points and PRNet and PRNet* have serious one-to-many matching problem.

Rigid transformation estimation evaluation. We also provide a comparison of transformation estimation, which is achieved by the Procrustes algorithm [42] based on the learned correspondence. Following [24], [25], we use the metrics of root mean square error (RMSE) and mean absolute error (MAE) between the ground truth and prediction of the Euler angle and translation vector, notated as RMSE(R), MAE(R), RMSE(t), and MAE(t). Among all the experimental settings in Table. II, our method achieves the best results on all metrics.

C. Ablation Studies

End-to-end training vs. Post-processing. We solve the zero-one assignment problem by end-to-end learning. Another more direct idea is to solve this non-convex problem by post-processing, *i.e.* learning the soft matching matrix and solving the permutation matrix during the test. From the comparison provided by Fig. 6, which is conducted on Surreal\SHREC, the end-to-end learning benefits the final results significantly because more accurate loss is calculated during the training.

IV. CONCLUSION

In this work, we advocate achieving one-to-one matching by learning the permutation matching matrix to tackle the dense correspondence estimation problem for 3D point clouds. Moreover, to guarantee the end-to-end learning and the accuracy of the calculated loss, an ingenious matching module has been designed in our method. Extensive experiments on both non-rigid and rigid 3D point cloud data have validated that ours achieved state-of-the-art performance. However, our method has limitations. Specifically, our method essentially determines the correspondences according to the similarity of the points. Thus, ours cannot deal with objects with strong symmetry, which is a stubborn problem in the community. In the future, we plan to extend our method to other dense correspondence estimation tasks, *e.g.* 2D-2D, 2D-3D.

REFERENCES

- [1] S. Deng and Q. Dong, “Ga-net: Global attention network for point cloud semantic segmentation,” *IEEE Signal Processing Letters*, vol. 28, pp. 1300–1304, 2021. [1](#)
- [2] S. Zhang, S. Cui, and Z. Ding, “Hypergraph spectral clustering for point cloud segmentation,” *IEEE Signal Processing Letters*, vol. 27, pp. 1655–1659, 2020. [1](#)
- [3] J.-E. Deschaud, “Imls-slam: scan-to-model matching based on 3d data,” in *Proceedings of the International Conference on Robotics and Automation*. IEEE, 2018, pp. 2480–2485. [1](#)
- [4] J. Zhang and S. Singh, “Loam: Lidar odometry and mapping in real-time,” in *Proceedings of Robotics: Science and Systems*, vol. 2, no. 9, 2014. [1](#)
- [5] E. Ramalho, E. Peixoto, and E. Medeiros, “Silhouette 4d with context selection: Lossless geometry compression of dynamic point clouds,” *IEEE Signal Processing Letters*, vol. 28, pp. 1660–1664, 2021. [1](#)
- [6] S. Gu, J. Hou, H. Zeng, and H. Yuan, “3d point cloud attribute compression via graph prediction,” *IEEE Signal Processing Letters*, vol. 27, pp. 176–180, 2020. [1](#)
- [7] E. Peixoto, “Intra-frame compression of point cloud geometry using dyadic decomposition,” *IEEE Signal Processing Letters*, vol. 27, pp. 246–250, 2020. [1](#)
- [8] G. Wan, X. Yang, R. Cai, H. Li, Y. Zhou, H. Wang, and S. Song, “Robust and precise vehicle localization based on multi-sensor fusion in diverse city scenes,” in *Proceedings of the International Conference on Robotics and Automation*. IEEE, 2018, pp. 4670–4677. [1](#)
- [9] Z. Li, J. Yuan, B. Jia, Y. He, and L. Xie, “An effective face anti-spoofing method via stereo matching,” *IEEE Signal Processing Letters*, vol. 28, pp. 847–851, 2021. [1](#)
- [10] B. Fan, K. Wang, Y. Dai, and M. He, “Rs-dpsnet: Deep plane sweep network for rolling shutter stereo images,” *IEEE Signal Processing Letters*, vol. 28, pp. 1550–1554, 2021. [1](#)
- [11] O. van Kaick, H. Zhang, G. Hamarneh, and D. Cohen-Or, “A survey on shape correspondence,” *Computer Graphics Forum*, vol. 30, no. 6, pp. 1681–1707, 2011. [1](#)
- [12] O. Litany, T. Remez, E. Rodolà, A. M. Bronstein, and M. M. Bronstein, “Deep functional maps: Structured prediction for dense shape correspondence,” in *Proceedings of the IEEE International Conference on Computer Vision*, 2017, pp. 5660–5668. [1, 3](#)
- [13] O. Halimi, O. Litany, E. Rodolà, A. M. Bronstein, and R. Kimmel, “Unsupervised learning of dense shape correspondence,” in *Proceedings of the IEEE Conference on Computer Vision and Pattern Recognition*, 2019, pp. 4370–4379. [1, 3](#)
- [14] N. Donati, A. Sharma, and M. Ovsjanikov, “Deep geometric functional maps: Robust feature learning for shape correspondence,” in *Proceedings of the IEEE Conference on Computer Vision and Pattern Recognition*, 2020, pp. 8589–8598. [1, 3, 4](#)
- [15] D. Boscaini, J. Masci, E. Rodolà, and M. M. Bronstein, “Learning shape correspondence with anisotropic convolutional neural networks,” in *Proceedings of the Advances in Neural Information Processing Systems*, 2016, pp. 3189–3197. [1](#)
- [16] F. Monti, D. Boscaini, J. Masci, E. Rodolà, J. Svoboda, and M. M. Bronstein, “Geometric deep learning on graphs and manifolds using mixture model cnns,” in *Proceedings of the IEEE Conference on Computer Vision and Pattern Recognition*, 2017, pp. 5425–5434. [1](#)
- [17] X. Liu, C. R. Qi, and L. J. Guibas, “Flownet3d: Learning scene flow in 3d point clouds,” in *Proceedings of the IEEE Conference on Computer Vision and Pattern Recognition*, 2019, pp. 529–537. [1, 3](#)
- [18] Y. Zeng, Y. Qian, Z. Zhu, J. Hou, H. Yuan, and Y. He, “Cornnet3d: Unsupervised end-to-end learning of dense correspondence for 3d point clouds,” in *Proceedings of the IEEE Conference on Computer Vision and Pattern Recognition*, 2021, pp. 6052–6061. [1, 3](#)
- [19] Z. Zhang, Y. Dai, and J. Sun, “Deep learning based point cloud registration: an overview,” *Virtual Reality and Intelligent Hardware*, vol. 2, no. 3, pp. 222–246, 2020. [1](#)
- [20] C. Choy, W. Dong, and V. Koltun, “Deep global registration,” in *Proceedings of the IEEE Conference on Computer Vision and Pattern Recognition*, 2020. [1](#)
- [21] X. Bai, Z. Luo, L. Zhou, H. Fu, L. Quan, and C.-L. Tai, “D3feat: Joint learning of dense detection and description of 3d local features,” in *Proceedings of the IEEE Conference on Computer Vision and Pattern Recognition*, 2020, pp. 6358–6366. [1](#)
- [22] Z. Gojcic, C. Zhou, J. D. Wegner, and A. Wieser, “The perfect match: 3d point cloud matching with smoothed densities,” in *Proceedings of the IEEE Conference on Computer Vision and Pattern Recognition*, 2019, pp. 5545–5554. [1](#)
- [23] Y. Wang and J. M. Solomon, “Prnet: Self-supervised learning for partial-to-partial registration,” in *Proceedings of the Advances in Neural Information Processing Systems*, 2019, pp. 8814–8826. [1, 3](#)
- [24] Y. Wang and J. M. Solomon, “Deep closest point: Learning representations for point cloud registration,” in *Proceedings of the IEEE International Conference on Computer Vision*, 2019, pp. 3523–3532. [1, 3, 4](#)
- [25] Z. J. Yew and G. H. Lee, “Rpm-net: Robust point matching using learned features,” in *Proceedings of the IEEE Conference on Computer Vision and Pattern Recognition*, June 2020. [1, 3, 4](#)
- [26] Z. Li, J. Tang, L. Zhang, and J. Yang, “Weakly-supervised semantic guided hashing for social image retrieval,” *International Journal of Computer Vision*, vol. 128, no. 8, pp. 2265–2278, 2020. [1](#)
- [27] Z. Li and J. Tang, “Weakly supervised deep metric learning for community-contributed image retrieval,” *IEEE Transactions on Multimedia*, vol. 17, no. 11, pp. 1989–1999, 2015. [1](#)
- [28] H. W. Kuhn, “The hungarian method for the assignment problem,” *Naval research logistics quarterly*, vol. 2, no. 1-2, pp. 83–97, 1955. [1, 2](#)
- [29] Y. Wang, Y. Sun, Z. Liu, S. E. Sarma, M. M. Bronstein, and J. M. Solomon, “Dynamic graph cnn for learning on point clouds,” *ACM Transactions on Graphics*, vol. 38, no. 5, pp. 1–12, 2019. [2](#)
- [30] A. Vaswani, N. Shazeer, N. Parmar, J. Uszkoreit, L. Jones, A. N. Gomez, Ł. Kaiser, and I. Polosukhin, “Attention is all you need,” in *Proceedings of the Advances in Neural Information Processing Systems*, 2017, pp. 5998–6008. [2](#)
- [31] G. Mena, D. Belanger, S. Linderman, and J. Snoek, “Learning latent permutations with gumbel-sinkhorn networks,” in *Proceedings of the The International Conference on Learning Representations*, 2018. [2](#)
- [32] T. Groueix, M. Fisher, V. G. Kim, B. C. Russell, and M. Aubry, “3d-coded: 3d correspondences by deep deformation,” in *Proceedings of the European Conference on Computer Vision*, 2018, pp. 235–251. [3](#)
- [33] F. Bogo, J. Romero, M. Loper, and M. J. Black, “FAUST: dataset and evaluation for 3d mesh registration,” in *Proceedings of the IEEE Conference on Computer Vision and Pattern Recognition*, 2014, pp. 3794–3801. [3](#)
- [34] D. Anguelov, P. Srinivasan, D. Koller, S. Thrun, J. Rodgers, and J. Davis, “SCAPE: shape completion and animation of people,” *ACM Transactions on Graphics*, vol. 24, no. 3, pp. 408–416, 2005. [3](#)
- [35] E. Arnold, O. Y. Al-Jarrah, M. Dianati, S. Fallah, D. Oxtoby, and A. Mouzakitis, “A survey on 3d object detection methods for autonomous driving applications,” *IEEE Transactions on Intelligent Transportation Systems*, vol. 20, no. 10, pp. 3782–3795, 2019. [3](#)
- [36] Z. Wu, S. Song, A. Khosla, F. Yu, L. Zhang, X. Tang, and J. Xiao, “3d shapenets: A deep representation for volumetric shapes,” in *Proceedings of the IEEE Conference on Computer Vision and Pattern Recognition*, 2015, pp. 1912–1920. [3](#)
- [37] S. Melzi, J. Ren, E. Rodolà, A. Sharma, P. Wonka, and M. Ovsjanikov, “Zoomout: spectral upsampling for efficient shape correspondence,” *ACM Transactions on Graphics*, vol. 38, no. 6, pp. 155:1–155:14, 2019. [3](#)
- [38] J. Ren, A. Poulernard, P. Wonka, and M. Ovsjanikov, “Continuous and orientation-preserving correspondences via functional maps,” *ACM Transactions on Graphics*, vol. 37, no. 6, pp. 248:1–248:16, 2018. [3](#)
- [39] M. Vestner, R. Litman, E. Rodolà, A. M. Bronstein, and D. Cremers, “Product manifold filter: Non-rigid shape correspondence via kernel density estimation in the product space,” in *Proceedings of the IEEE Conference on Computer Vision and Pattern Recognition*, 2017, pp. 6681–6690. [3](#)
- [40] J. Roufousse, A. Sharma, and M. Ovsjanikov, “Unsupervised deep learning for structured shape matching,” in *Proceedings of the IEEE International Conference on Computer Vision*, 2019, pp. 1617–1627. [3](#)
- [41] P. Besl and H. McKay, “A method for registration of 3-d shapes,” *IEEE Transactions on Pattern Analysis and Machine Intelligence*, vol. 14, no. 2, pp. 239–256, 1992. [3](#)
- [42] J. C. Gower, “Generalized procrustes analysis,” *Psychometrika*, vol. 40, no. 1, pp. 33–51, 1975. [4](#)